Canonical Typicality of Energy Eigenstates of an Isolated Quantum System

Anatoly Dymarsky[1] and Hong Liu[2]

[1] *Skolkovo Institute of Science and Technology, Skolkovo Innovation Center, Moscow 143026 Russia*
[2] *Center for Theoretical Physics, Massachusetts Institute of Technology, Cambridge, MA 02139*

(Dated: November 23, 2015)

Currently there are two main approaches to describe how quantum statistical physics emerges from an isolated quantum many-body system in a pure state: Canonical Typicality (CT) and Eigenstate Thermalization Hypothesis (ETH). These two approaches has different but overlapping areas of validity, phenomenology and set of physical outcomes. In this paper we discuss the relation between CT and ETH and propose a formulation of ETH in terms of the reduced density matrix. We provide strong numerical evidences for the proposal.

I. CANONICAL TYPICALITY OF ENERGY EIGENSTATES

During the last two decades there has been significant progress in understanding how quantum statistical physics emerges from the dynamics of an isolated quantum many-body system in a pure state. One important recdent development is the notion of "Canonical Typicality" which states that a typical state of a small subsystem is well approximated by the microcanonical ensemble [1, 2]. More explicitly, for a random pure state Ψ from an energy shell $(E, E+\delta E)$,

$$|\Psi\rangle = \sum_n c_n |E_n\rangle, \qquad E_n \in (E, E+\delta E), \tag{1}$$

the corresponding reduced density matrix $\rho^A_\Psi \equiv \mathrm{Tr}_{\bar{A}}|\Psi\rangle\langle\Psi|$ for a sufficiently small subsystem A (whose complement is denoted as $\bar{A}$) satisfies

$$\rho^A_\Psi \approx \rho^A_{\rm micro}, \tag{2}$$

where $\rho^A_{\rm micro} = \mathrm{Tr}_{\bar{A}}\,\rho_{\rm micro}$ is the reduction of the microcanonical density matrix $\rho_{\rm micro}$ defined for the same energy shell. As usual one assumes that the system is large and the shell width δE is very small compared with E, but much larger than typical level spacings. Canonical typicality explains emergence of statistical ensembles. It is, however, a purely kinematic statement which does not say anything about whether or how a non-equilibrium initial state thermalizes [3].

Another development is the so-called Eigenstate Thermalization Hypothesis (ETH) [4–6] which conjectures that for a quantum chaotic system a finitely excited energy eigenstate behaves thermally when probed by few-body operators. More explicitly, for a few-body operator $\mathcal{O}$, ETH postulates that

$$\mathcal{O}_E \equiv \langle E|\mathcal{O}|E\rangle = f_\mathcal{O}(E) + e^{-O(N)}, \tag{3}$$

$$\mathcal{O}_{E_1E_2} \equiv \langle E_1|\mathcal{O}|E_2\rangle \sim e^{-O(N)}, \qquad E_1 \neq E_2, \tag{4}$$

where $|E\rangle$ denotes an energy eigenstate, $f_\mathcal{O}(E)$ is a smooth function of E, and N is the total number of degrees of freedom. ETH is a dynamical statement; it does not apply to integrable or many-body localized systems.

For systems satisfying ETH, emergence of microcanonical ensemble for the pure state (1) is evident from (3)–(4),

$$\langle\Psi|\mathcal{O}|\Psi\rangle = \sum_n |c_n|^2 \mathcal{O}_{E_n} + \sum_{m\neq n} c_n^* c_m \mathcal{O}_{E_nE_m} \approx f_\mathcal{O}(E)\ ,$$
$$\langle\mathcal{O}\rangle_{\rm micro} \approx f_\mathcal{O}(E)\ . \tag{5}$$

We have used above that for a random state coefficients c_n are uncorrelated with $\mathcal{O}_{E_mE_n}$ hence the contribution of the off-diagonal terms is of order $e^{-O(N)}$ and can be neglected.

CT is a general statement as it does not refer to Hamiltonian and thus applies universally to all systems. ETH is, however, a stronger statement as it implies emergence of microcanonical ensemble not only for random Ψ, but for a wider class of states, include linear combination of a few energy eigenstates. It also ensures the eventual thermalization of all non-equilibrium initial states with sufficiently small energy fluctuations. To see this, consider starting with an initial state Ψ for which (5) is not satisfied due to a special choice of c_n such that the off-diagonal terms contribute significantly. Time evolution will then introduce random relative phases between all coefficients c_n. Eventually (5) will be satisfied which means the system has reached the state of microscopic equilibrium (until recurrences).

At a heuristic level, canonical typicality can be understood as a consequence of entanglement between a sufficiently small subsystem and its complement [2]. While the full system evolves unitarily, a small subsystem can behave thermally as its complement essentially plays the role of a large bath. This is also reminiscent of a result of Page [7] which says that the average entanglement entropy of a small subsystem A in a pure random state is given by $\log\mathcal{N}_A$ were $\mathcal{N}_A$ is the dimension of the Hilbert space of A.

In the context of ETH, the need to restrict to few-body operators can be understood in a similar way as the few-body operators probe only a small part of the total system. That ETH applies only to chaotic systems follows from the general picture of CT; only for chaotic systems are energy eigenstates "random enough" to be typical. In other words the Eigenstate Thermalization Hypothesis could be understood as the expectation that for a general interacting system energy eigenstates would

be complex enough to be typical. This perspective thus motivates us to formulate ETH in terms of the reduced density matrix of a subsystem, analogous to the formulation of CT (2).

Split a system into subsystem A and its complement $\bar{A}$ with the corresponding degrees of freedom given by N_A and $N_{\bar{A}}$ respectively. We first consider $N_A \ll N_{\bar{A}} \approx N$, with N being the total number of degrees of freedom. In analogue with (3) we postulate that:

(i) all matrix elements of ρ_E^A, defined as

$$\rho_E^A = \mathrm{Tr}_{\bar{A}} |E\rangle\langle E| \tag{6}$$

are smooth functions of E up to corrections of order $e^{-O(N)}$.

(ii) all matrix elements of the "off-diagonal" reduced matrix are exponentially small in the total system size, i.e.

$$\rho^A_{E_1E_2} \equiv \mathrm{Tr}_{\bar{A}} |E_1\rangle\langle E_2| \sim e^{-O(N)}, \qquad E_1 \neq E_2 \ . \tag{7}$$

Note that (i) immediately implies

$$\rho_E^A = \rho^A_{\rm micro} + e^{-O(N)} \tag{8}$$

and for a random pure state (1), (i) and (ii) ensure

$$\rho_\Psi^A \approx \rho^A_{\rm micro}. \tag{9}$$

There are various advantages to formulate ETH in terms of reduced density matrices of subsystems. Firstly the density matrix formulation makes entanglement properties between a subsystem and its complement more manifest. One can readily use it to generalize the statements (3) regarding few-body local operators to non-local observables such as entanglement entropy, Renyi entropies, negativity and etc. In particular, it gives a natural interpretation of the thermal entropy as the entanglement entropy of a subsystem (see [8, 9] for recent discussions). Secondly, as we will discuss immediately below, the density matrix formulation provides a direct way to introduce the concept of local temperature and local canonical ensemble. Thirdly, while for systems with a finite Hilbert space the density matrix and operator formulation are mathematically equivalent, for systems with an infinite local Hilbert space or for region A which scales to infinity in the thermodynamical limit, the density matrix formulation provides a more precise definition for observables which satisfy ETH.

A formulation of ETH from the density matrix perspective has been recently discussed in [10] in the thermodynamical limit $N_{\bar{A}} \to \infty$ and some of the above points were also emphasized along with others.

Besides $\rho^A_{\rm micro}$ it is also natural to compare ρ_E^A with the reduced density matrices for other statistical ensembles. Of particular interests are the canonical ensemble for the whole system,

$$\rho_C^A = \frac{\mathrm{Tr}_{\bar{A}}\, e^{-\beta H}}{\mathrm{Tr}\ e^{-\beta H}}, \tag{10}$$

and the local canonical ensemble for the subsystem A,

$$\rho_G^A = \frac{e^{-\beta H_A}}{\mathrm{Tr}_A\ e^{-\beta H_A}}. \tag{11}$$

Here the Hamiltonian of the subsystem is the restriction of the Hamiltonian $H_A = \mathrm{Tr}_{\bar{A}} H$. In (10) β is to be chosen so that the average energy of the total system is E. In (11), β can be interpreted as a local temperature of A (see also [11, 12]). There appears to be no canonical choice for β in this case. One choice is to define it to be the same as in (10), as we will always do below. In the thermodynamic limit $N_{\bar{A}} \to \infty$ with N_A kept fixed, the standard saddle point approximation argument gives

$$\rho^A_{\rm micro} = \rho_C^A + O(N^{-1}), \quad \Rightarrow \quad \rho_E^A = \rho_C^A + O(N^{-1}), \tag{12}$$

where we have used (8). Note, that in contrast to (8), the difference between ρ_E^A and ρ_C^A is only power suppressed. Since even in the thermodynamical limit the trace distance $\left|\left|\rho_C^A - \rho_G^A\right|\right|_1$ remains finite [11],

$$\rho_C^A - \rho_G^A \neq 0 \quad \Rightarrow \quad \rho_E^A \neq \rho_G^A, \tag{13}$$

for fixed N_A and $N_{\bar{A}} \to \infty$.

It is also of interests to consider an alternative thermodynamic limit keeping the ratio

$$0 < p = \frac{N_A}{N} < \frac{1}{2} \tag{14}$$

fixed and taking $N \to \infty$. In this limit, while we still expect ρ_E to approach $\rho_{\rm micro}$ at the level of individual matrix elements, the story is more intricate. The reason is that typical matrix elements of ρ_E^A scale as

$$\rho_E^A \sim \mathcal{N}_A^{-1} \sim e^{-O(N)}, \tag{15}$$

so in order to make sense of (8) we need to worry about the prefactor before N in the exponential. Equation (8) can be rewritten in terms of the size of the full Hilbert space $\mathcal{N}$,

$$\rho_E^A = \rho^A_{\rm micro} + O\left(\mathcal{N}^{-c}\right), \tag{16}$$

and would have a sensible limit only if $c > p$, where we used $\mathcal{N}_A \sim \mathcal{N}^p$. For a maximally chaotic system, we expect $c = \frac{1}{2}$, hence for such theories the condition $c > p$ is always satisfied.

When both N_A and N are large we expect ρ_E^A should have a semi-classical description. We conjecture that to leading order in N, ρ_E^A will be diagonal in the eigenbasis $|\mathcal{E}_a\rangle$ of H_A with the diagonal elements given by

$$\langle \mathcal{E}_a|\rho_E^A|\mathcal{E}_a\rangle = \langle \mathcal{E}_a|\rho^A_{\rm micro}|\mathcal{E}_a\rangle = \frac{\Omega_{\bar{A}}(E - \mathcal{E}_a)}{\Omega(E)}, \tag{17}$$

where Ω_A, Ω are the density of states for H_A, H respectively. The expression (17) reflects the quasiclassical expectaion that the probability to find the subsystem in a state with energy $\mathcal{E}_a$ is proportional to the number of such

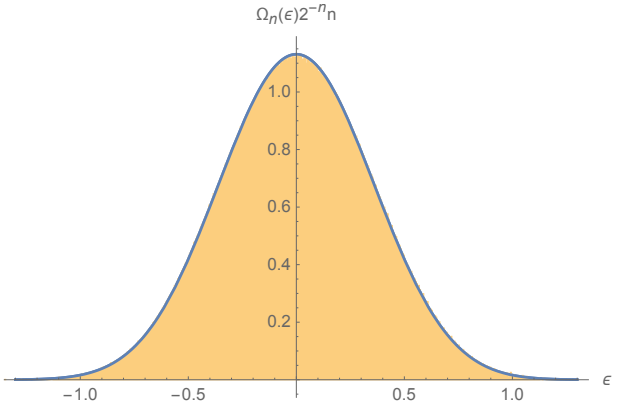

FIG. 1. The density of states of the spin chain system for $g = 1.05, h = 0.1, n = 17$. The horizontal axis is energy per site $\epsilon = E/n$. The yellow bars which fill the plot are the histogram for the density of states. The blue solid line is a theoretical fit by the binomial distribution function. The corresponding parameters can be found in the Appendix A.

states. Also for Hamiltonians with local interactions, when N_A, N are large, we have $H = H_A + H_{\bar{A}} + o(N_A)$, and one would expect $\rho_C^A = \rho_G^A$ at leading order in N_A. As a consistency check one can readily see that following from (17).

Finally note that from (17), in the limit of (14) with fixed nonzero p

$$\rho_E^A = \rho_{\text{micro}}^A \neq \rho_C^A = \rho_G^A \ . \tag{18}$$

For example, their Renyi entropies are different (although the entanglement entropy of ρ_E^A does coincide with that of $\rho_C^A = \rho_G^A$ at leading order). See Appendix C for details. Also note that when $p \to 0$, $\rho_E^A = \rho_C^A = \rho_G^A$ to leading order in N_A. A similar observation was previously made in [14] in a context of a particular model.

For the rest of the paper we provide numerical supports for (8), (7) and (17) in a one-dimensional spin chain model. In particular, we will provide strong numerical evidence for the exponential suppression in (7)–(8).

II. NUMERICAL RESULTS

In this section we test the hypothesis (i) and (ii) for the density matrix formulation of ETH discussed in the introduction by numerically simulating a one-dimensional spin chain.

We consider an open Ising spin chain with a transverse and longitudinal magnetic field

$$H = -\sum_{i=1}^{n-1} \sigma_z^i \otimes \sigma_z^{i+1} + g\sum_{i=1}^{n} \sigma_x^i + h\sum_{i=1}^{n} \sigma_z^i \ , \tag{19}$$

which is known to exhibit chaotic behavior unless one of the coupling constants g or h is zero. We solve the system by exact diagonalization for $g = 1.05$ and various

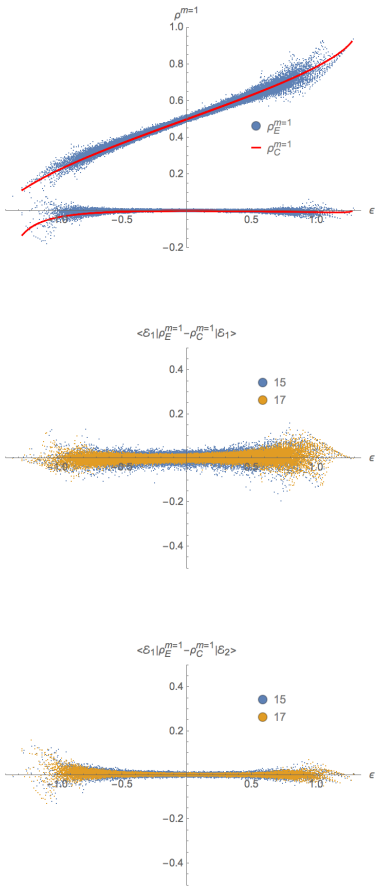

FIG. 2. **Top:** Diagonal (upper) and off-diagonal (lower) elements of the reduced density matrix ρ_E^A consisting of $m = 1$ spin in the eigenbasis of H_A as a function of energy-per-site $\varepsilon = \mathcal{E}/n$ for $g = 1.05, h = 0.1$. The red solid lines are the numerical values for ρ_C^A of (10). Note that the off-diagonal elements of ρ_C^A are nonzero. **Center and Bottom:** The difference $\rho_E^A - \rho_C^A$ for diagonal and off-diagonal matrix elements. Note that convergence of ρ_E^A to ρ_C^A is slow as discussed in (12) their difference is controlled by $1/n$.

values of h ranging from $h = 0$ to $h = 1$. For this model, the range of the energy spectrum is roughly from $-n$ to n where n is the total number of spins. The density of states for a particular choice of parameters is shown in Fig. 1. We will focus on the behavior for E near the central value $E = 0$ of the spectrum, which correspond to highly excited states.

We will denote as m the number of consecutive spins in subsystem A, and express ρ_E^A and ρ_{E_1,E_2}^A in terms of the eigenbasis $|\mathcal{E}_a\rangle$ of H_A (index a is ordered such that $\mathcal{E}_a > \mathcal{E}_b$ for $a > b$). Under the assumption that the elements of ρ_E^A are smooth functions of E, near $E = 0$ we can Taylor expand it as

$$\rho_E^A = \varrho + \varrho' E + \cdots \tag{20}$$

where ϱ and ϱ' are some matrices. For finite n, we expect

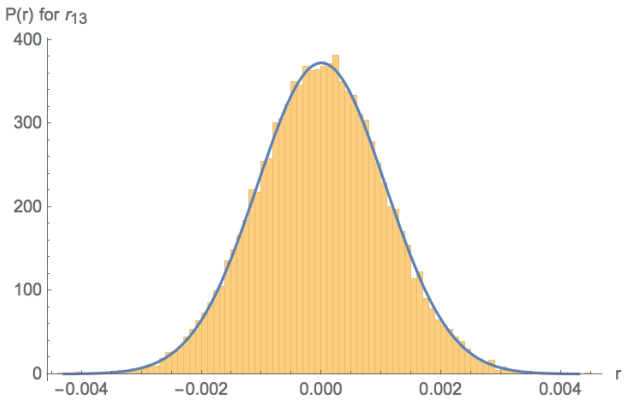

FIG. 3. Probability distribution $P(r)$ for the deviation $r_{13}(E)$ of a matrix element $\langle \mathcal{E}_1|\rho_E^{m=2}|\mathcal{E}_3\rangle$ from the microcanoncal mean with $h = 0.1$, superimposed with a Gaussian distribution fit. The vertical axis is the number of energy eigenstates within the energy shell ΔE with a particular value of r_{13}. All matrix elements of $\rho_E^{m=1,2,3}$ show almost identical behavior.

fluctuations around (20), as in Fig. 2, where we give the values of ρ_E^A and compare them with ρ_C^A. A trend to converge with increasing n is already visible in the plot, but note that the asymptotic convergence rate is expected to be slow, of order $1/n$.

To study convergence of ρ_E^A to its microcanonical average ρ_{micro}^A quantitatively we introduce an energy shell of width ΔE and calculate ϱ, ϱ' from linearly approximating ρ_E^A using least squares method for all $|E\rangle$ within the shell. We are then interested in the "probability distributions" $P(r)$ of the matrix elements

$$r_{ab}(E) = \langle \mathcal{E}_a|\rho_E^A - (\varrho + \varrho' E)|\mathcal{E}_b\rangle. \tag{21}$$

In Fig. 3, we show the distribution $P(r)$ for one of the matrix elements for $m = 2$ spins, with the distributions for other matrix elements for $m = 1, 2, 3$ almost identical. Fig. 3 shows that $P(r)$ is well approximated by a Gaussian.

The standard deviation σ_n of the Gaussian distribution fit shows a robust independence of ΔE as far as the energy shell includes large enough number of states (as in usual microcanonical average). Remarkably, we find that σ_n decreases exponentially with the system size n for all matrix elements of ρ_E^A for $m = 1, 2, 3$ and for all values of coupling $h > 0$. With $P(r)$ well described by the normal distribution, exponential convergence of variance σ_n implies all deviations $r_{ab}(E)$ will approach zero as n increases. We also note that there is no substantial qualitative difference in the convergence rate

$$\alpha = d \log \sigma_n / dn \tag{22}$$

for different matrix elements of $\rho_E^{m=1,2,3}$, see fig. 4. We thus find strong evidence of hypothesis (i) and (8) for the

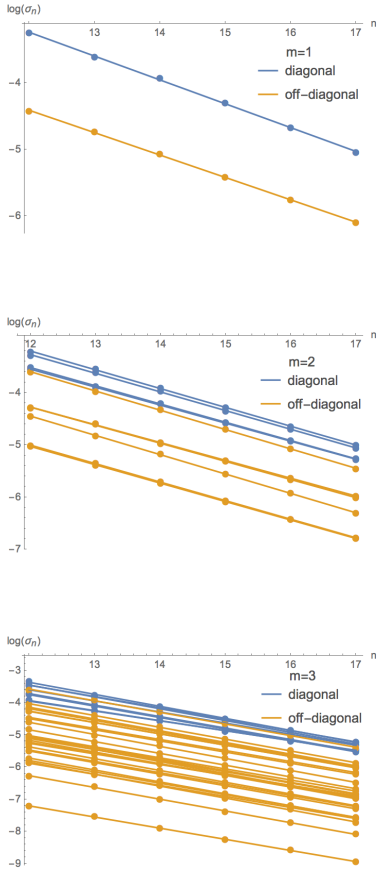

FIG. 4. Linear behavior of $\log(\sigma_n)$ as a function of system size n for matrix elements r_{ab} for $m = 1, 2, 3$, $h = 0.1$ and $n = 17$. Because of the approximate equality $\rho_C \approx \rho_G$ the typical magnitude of the diagonal terms of ρ_E is much larger than the off-diagonal ones. There is no qualitative difference between different matrix elements.

density matrix formulation of ETH. In particular, our results explain strong version of ETH recently discussed in [15].

While the convergence rate α is approximately the same for all matrix elements of ρ_E^A and different choices of A, α is strongly dependent on h (for fixed g). At the integrable point $h = 0$, α appears to be zero and rapidly increases with h. Even for very small positive h the decrease of σ_n is exponential, albeit with a small rate. In other words ETH holds for all values of h except for $h = 0$ but for small h ETH behavior becomes appreciable only for sufficiently large (and not necessarily numerically accessible) n. This behavior is consistent with previous studies of ETH near integrable point [16, 17]. At around $h \simeq 0.1$ the convergence rate approaches its maximal numerically observed value $\alpha \simeq -\frac{1}{2}\log 2$, which means the magnitude of the deviation $r(E)$ scales with the dimension of Hilbert space $\mathcal{N}$ as $\mathcal{N}^{-\frac{1}{2}}$. The same scaling may be expected from a random Hamiltonian, which leads us

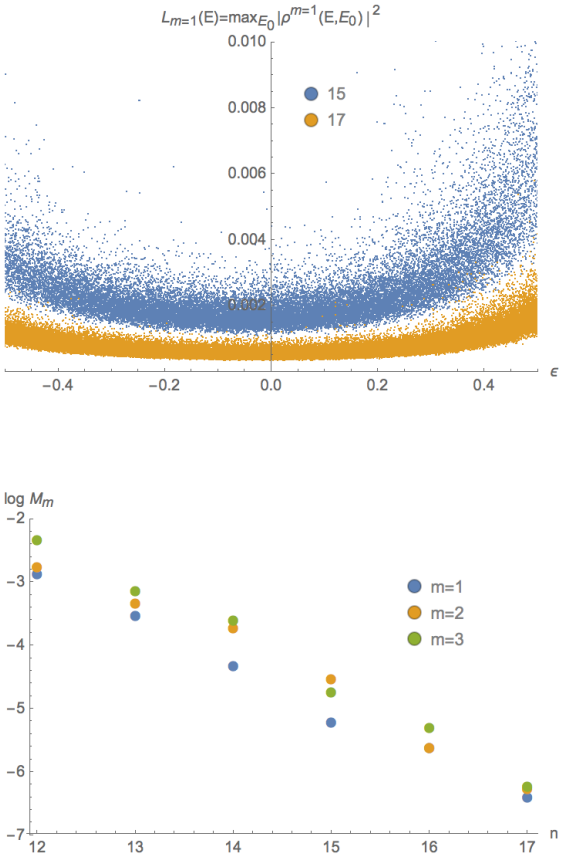

FIG. 5. **Top:** Plot of $L_A(E)$ v.s. $\epsilon = E/N$ for $n = 15$ and $n = 17$. **Bottom:** $M_{m=1,2,3}$ all decrease exponentially with n. Here $E_{\max}$ is chosen to be equal $0.1n$ and $h = 0.1$.

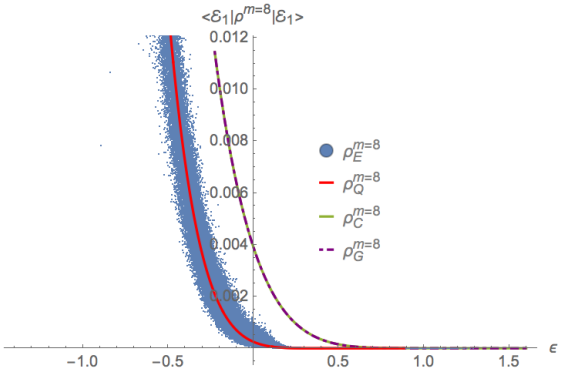

FIG. 6. Comparison of matrix elements of $\rho_E^A, \rho_C^A, \rho_G^A$ and the quasiclassical result (17) which we refer to as ρ_Q^A. Blue dots are matrix elements $\langle\mathcal{E}_1|\rho_E^{m=8}|\mathcal{E}_1\rangle$ as a function of energy per site $\varepsilon = \mathcal{E}/n$ for $h = 0.1$ and $n = 17$. We see that $\langle\mathcal{E}_1|\rho_E^{m=8}|\mathcal{E}_1\rangle$ follows the semi-classical result $\langle\mathcal{E}_1|\rho_Q^{m=8}|\mathcal{E}_1\rangle$ as given by (17) well, while differs significantly from $\langle\mathcal{E}_1|\rho_C^{m=8}|\mathcal{E}_1\rangle \approx \langle\mathcal{E}_1|\rho_G^{m=8}|\mathcal{E}_1\rangle$, which lie on top of each other. Other matrix elements show similar behavior.

to believe $\sigma(\mathcal{N}) \sim \mathcal{N}^{-\frac{1}{2}}$ is the fastest possible rate of convergence which corresponds to "maximally chaotic" systems.

Now let us examine (7). To quantify smallness of $\rho^A_{EE'}$ we introduce the norm

$$|\rho^A_{EE'}| = \sqrt{\mathrm{Tr}_A\left[(\rho^A_{EE'})^\dagger \rho^A_{EE'}\right]}\ . \tag{23}$$

The corresponding variance can be calculated in full generality for any quantum system,

$$\sigma^2_{E_0} = \frac{1}{\mathcal{N}}\sum_E |\rho^A_{EE_0}|^2 = \frac{\mathcal{N}_A}{\mathcal{N}}\ , \tag{24}$$

where $\mathcal{N}_A$ is the dimension of $\mathcal{H}_A$ (see Appendix B for a proof). In the case of spin-chain $\mathcal{N}_A/\mathcal{N} = e^{-(n-m)\log 2}$. Equation (24) implies that on average $|\rho^A_{EE'}| \sim \mathcal{N}^{-\frac{1}{2}}$, but there remains the possibility that a small number (of order $O(\mathcal{N}_A)$) of $|\rho^A_{EE'}|$ is of order $O(1)$, while the others are further suppressed from $\mathcal{N}^{-\frac{1}{2}}$. To eliminate this possibility, we further examine the following quantity

$$M_A \equiv \max_{|E|<E_{\max}} \max_{E_0} |\rho^A_{EE_0}|^2, \tag{25}$$

where for a given E we first scan E_0 to find the maximal value $L_A(E) \equiv \max_{E_0} |\rho^A_{EE_0}|^2$, and then find $M_A = \max L_A(E)$ by scanning all values of E within the window $|E| < E_{\max}$. The restriction to $|E| < E_{\max}$ is necessary as ETH is only expected to apply to the finitely excited states, not to the states from the edges of the spectrum. This is manifest in the upper plot of Fig. 5. The bottom plot of Fig. 5 indicates that M_A decreases exponentially with n. Thus we have found strong numerical support for (7).

Finally, we consider the behavior of ρ^A_E when A becomes comparable to $\bar{A}$ to probe validity of (17). Clearly to probe this regime numerically is much more challenging. Here our numerical results are nevertheless quite suggestive. We consider subspace A consisting of 8 leftmost consecutive spins with $n = 17$ and $h = 0.1$. The numerical results given in Fig. 6 show that ρ^A_E follows (17) pretty well while significantly differs from $\rho^A_C \approx \rho^A_G$.

Acknowledgements

This work is supported by funds provided by MIT-Skoltech Inititative. We would like to thank the University of Kentucky Center for Computational Sciences for computing time on the Lipscomb High Performance Computing Cluster.

Appendix A: Density of States

A non-interacting spin-chain with $J = 0$ exhibits the discreet density of states describe by the binomial distri-

bution. Once the interaction is introduced the density of states $\Omega(E)$ will become continuous, yet we still might expect the binomial distribution to be a good theoretical fit. For the spin-chain in question (19) we start with the ansatz

$$\Omega_n(E) = \frac{\kappa\, n!}{(n/2-\kappa\, E)!(n/2+\kappa\, E)} \tag{A1}$$

for some κ and notice that it is properly normalized for any value of κ with an exponential precision, $\int dE\, \Omega_n(E) \simeq 2^n$. We fix the parameter κ using the value of the second moment

$$\int dE\, E^2\, \Omega_n(E) \simeq 2^{n-2} n\kappa^{-2} = \mathrm{Tr}\, H^2. \tag{A2}$$

The latter could be calculated exactly from (19) yielding $\kappa = \frac{1}{2}\left(g^2+h^2+1-1/n\right)^{-1/2}$.

Appendix B: Variance

Consider the variance

$$\sigma^2_{E_0} = \frac{1}{\mathcal{N}} \sum_E |\rho^A_{EE_0}|^2 \tag{B1}$$

for some fixed E_0 and $\mathcal{N}$ is the dimension of the full Hilbert space. Since $|E\rangle$ is a complete basis,

$$\sum_E \langle E|\Psi_1\rangle\langle\Psi_2|E\rangle = \langle\Psi_2|\Psi_1\rangle. \tag{B2}$$

Now let us introduce a basis in the Hilbert space $|a,\alpha\rangle = |a\rangle\otimes|\bar a\rangle$ associated with the decomposition $\mathcal{H} = \mathcal{H}_A\otimes\mathcal{H}_{\bar A}$. Then

$$\langle a|\rho^A_{EE_0}|b\rangle = \sum_{\bar a} \langle a,\bar a|E\rangle\langle E_0|b,\bar a\rangle \tag{B3}$$

and

$$\sigma^2_{E_0} = \frac{1}{\mathcal{N}} \sum_E \sum_{a,b} \sum_{\bar a,\bar b} \langle a,\bar a|E\rangle\langle E_0|b,\bar a\rangle\langle b,\bar b|E_0\rangle\langle E|a,\bar b\rangle.$$

Now we use (B2) to get

$$\sigma^2_{E_0} = \frac{\mathcal{N}_A}{\mathcal{N}} \sum_a \sum_{\bar a} \langle E_0|a,\bar a\rangle\langle a,\bar a|E_0\rangle = \frac{\mathcal{N}_A}{\mathcal{N}}. \tag{B4}$$

Appendix C: Semi-classical expression

In this Appendix we discuss properties of (17) in the limit when (14) is kept fixed and $N\to\infty$. In particular we show that at the leading order in $1/N$ the Von Neumann entropy associated with ρ^A_E, which is given by (17), is the same as for ρ^A_G, despite the inequality (18).

In the limit $N_A\to\infty$ we can treat the energy levels $\mathcal{E}_a$ of A as a continuous variable $\mathcal{E}$, in terms of which

$$\Omega(E) = \int d\mathcal{E}\, \Omega_A(\mathcal{E})\Omega_{\bar A}(E-\mathcal{E}) \tag{C1}$$

where Ω_A is the density of states for A. Now introduce

$$\log\Omega_A \equiv \mathcal{S}_A, \qquad \log\Omega_{\bar A} \equiv \mathcal{S}_{\bar A}, \qquad \log\Omega \equiv \mathcal{S}, \tag{C2}$$

with the conventional expectation that the density of states grows exponentially with the volume,

$$\mathcal{S}_A \propto N_A, \qquad \mathcal{S}_{\bar A} \propto N_{\bar A}, \qquad \mathcal{S} \propto N\ . \tag{C3}$$

Since both $\mathcal{S}_A$ and $\mathcal{S}_{\bar A}$ are proportional to N we can use the saddle point approximation in (C1) to obtain

$$\mathcal{S}(E) = \mathcal{S}_A(\bar{\mathcal{E}}_A) + \mathcal{S}_{\bar A}(\bar{\mathcal{E}}_{\bar A}) \tag{C4}$$

where $\bar{\mathcal{E}}_A$ and $\bar{\mathcal{E}}_{\bar A}$ are determined by

$$\bar{\mathcal{E}}_A + \bar{\mathcal{E}}_{\bar A} = E, \qquad \left.\frac{\partial\mathcal{S}_A}{\partial\mathcal{E}}\right|_{\bar{\mathcal{E}}_A} = \left.\frac{\partial\mathcal{S}_{\bar A}}{\partial\mathcal{E}}\right|_{\bar{\mathcal{E}}_{\bar A}}\ . \tag{C5}$$

Using saddle point approximation for the canonical ensemble of the whole system we we recover the conventional relation between the inverse temperate β and the mean energy E,

$$\beta = \frac{\partial\mathcal{S}(E)}{\partial E}. \tag{C6}$$

Together with (C4)–(C5) this implies

$$\beta = \left.\frac{\partial\mathcal{S}_A}{\partial\mathcal{E}}\right|_{\bar{\mathcal{E}}_A} = \left.\frac{\partial\mathcal{S}_{\bar A}}{\partial\mathcal{E}}\right|_{\bar{\mathcal{E}}_{\bar A}}\ . \tag{C7}$$

Then it follows in a standard way that the entropy S^A_G associated with

$$\rho^A_G(\mathcal{E}) \simeq e^{-\beta(\mathcal{E}-\bar{\mathcal{E}}_A)-\mathcal{S}_A(\bar{\mathcal{E}}_A)} \tag{C8}$$

is simply $S^A_G = \mathcal{S}_A(\bar{\mathcal{E}}_A)$.

With help of (C4) one can rewrite (17) as follows,

$$\rho^A_E(\mathcal{E}) \simeq e^{\mathcal{S}_{\bar A}(E-\mathcal{E})-\mathcal{S}_{\bar A}(E-\bar{\mathcal{E}}_A)-\mathcal{S}_A(\bar{\mathcal{E}}_A)} \tag{C9}$$

and the corresponding entropy S^A_E is then given by

$$S^A_E = -\operatorname*{Tr}_A \rho^A_E \log\rho^A_E = \mathcal{S}_A(\bar{\mathcal{E}}_A) = S^A_G\ . \tag{C10}$$

From (C8) and (C9) one can readily see the Renyi entropies for ρ^A_E are different from those of ρ^A_G.

[1] S. Goldstein, J. Lebowitz, R. Tumulka, and N. Zanghi, "Canonical typicality," Physical review letters 96, no. 5 (2006): 050403, [arXiv:cond-mat/0511091].

[2] S. Popescu, A. Short , A. Winter, "Entanglement and the foundations of statistical mechanics," Nature Physics, (2006): 2(11), 754-758, [arXiv:quant-ph/0511225].

[3] Nevertheless some kinematic statements can be made, see N. Linden, S. Popescu, A. Short, and A. Winter, "Quantum mechanical evolution towards thermal equilibrium," Physical Review E 79, no. 6 (2009): 061103, [arXiv:0812.2385] and S. Goldstein, J. Lebowitz, C. Mastrodonato, R. Tumulka, and N. Zanghi, " Approach to thermal equilibrium of macroscopic quantum systems," Physical Review E, 81(1), (2010): 011109, [arXiv:0911.1724].

[4] J. Deutsch, "Quantum statistical mechanics in a closed system," Physical Review A 43, no. 4 (1991): 2046.

[5] Srednicki, "Chaos and quantum thermalization," Physical Review E 50, no. 2 (1994): 888.

[6] M. Rigol, V. Dunjko, and M. Olshanii, "Thermalization and its mechanism for generic isolated quantum systems," Nature, (2008): 452(7189), 854-858, [arXiv:0708.1324].

[7] D. N. Page, "Average entropy of a subsystem," Phys. Rev. Lett. **71**, 1291 (1993) [gr-qc/9305007].

[8] J. Deutsch, "Thermodynamic entropy of a many-body energy eigenstate," New Journal of Physics 12, no. 7 (2010): 075021, [arXiv:0911.0056].

[9] J. Deutsch, H. Li, and A. Sharma, "Microscopic origin of thermodynamic entropy in isolated systems," Physical Review E 87, no. 4 (2013): 042135, [arXiv:1202.2403].

[10] J. R. Garrison and T. Grover, "Does a single eigenstate encode the full Hamiltonian?," [arXiv:1503.00729].

[11] Ferraro, Alessandro and García-Saez, Artur and Acín, Antonio, "Intensive temperature and quantum correlations for refined quantum measurements", EPL (Europhysics Letters), v. 98, **1**, 2012, [arXiv:1102.5710].

[12] Kliesch, M., et al. "Locality of temperature." Physical Review X 4.3 (2014): 031019.

[13] S. Hernández-Santana, A. Riera, K. Hovhannisyan, M. Perarnau-Llobet, L. Tagliacozzo, A. Acín "Locality of temperature in spin chains," New J. Phys. 17, 085007 (2015)

[14] H. Tasaki, "From quantum dynamics to the canonical distribution: general picture and a rigorous example," Physical review letters 80, no. 7 (1998): 1373, [arXiv:cond-mat/9707253].

[15] H. Kim, T. Ikeda, and D. Huse, "Testing whether all eigenstates obey the Eigenstate Thermalization Hypothesis," Physical Review E, (2014): 90(5), 052105, [arXiv:1408.0535].

[16] M. Rigol, "Breakdown of thermalization in finite one-dimensional systems," Physical review letters 103, no. 10 (2009): 100403, [arXiv:0904.3746].

[17] L. Santos, M. Rigol, "Onset of quantum chaos in one-dimensional bosonic and fermionic systems and its relation to thermalization," Physical Review E 81, no. 3 (2010): 036206, [arXiv:0910.2985].